

Design and Implementation of an SMA-Actuated Jumping Robot

Thanhtam Ho and Sangyoon Lee

Abstract—The jumping locomotion can be quite a useful way for ground robots because it can provide a high locomotion speed and energy efficiency. We report in this paper the design, simulation, and preliminary experimental results of a jumping robot that is 150 mm long. The robot design is inspired by the structure of vertebrates' musculoskeletal system and the function of muscles that are used for the jumping motion. A few essential muscles are applied to our robot in the form of shape memory alloy (SMA) wires. The jumping motion of a computer model is simulated to find a suitable pattern of SMA wire activation. The parameters obtained from the simulation are applied to a robot prototype in experiments. Experimental results show that the forward distance obtained from the jumping experiment is comparable to the simulation result.

I. INTRODUCTION

LEGGED robots are known to have several advantages over wheeled ones in the ground locomotion. The most obvious advantage of legged robots is the mobility [1]. The ability of overcoming obstacles is another significant strength of legged robots.

Among various locomotion gaits employed by the legged robots, the jumping gait has clear advantages in terms of the travel speed and the energy efficiency. The jumping locomotion can help animals or insects to overcome obstacles, and hence they can be less dependable on the type of terrain. Therefore jumping creatures have inspired robotics scientists and engineers to investigate and develop jumping mechanisms. The efforts to mimic the musculoskeletal systems of biological creatures can be found in the multi-DOF (degree of freedom) jumping robot [2], the Mowgli robot [3], and the rabbit robot [4].

The jumping gait entails an extremely large force in a short time. Therefore, the pneumatic actuator is often chosen for the jumping mechanism. The pneumatic actuator has a larger power-to-weight ratio than the electromagnetic motor [5]. In addition, the pneumatic actuator produces the linear motion, which is closer to the behavior of muscles than the rotation of the electromagnetic motor. However, the pneumatic actuator tends to make robots heavier and larger due to the complexity of pneumatic systems and its power supply source.

SMA (shape memory alloy) has an enormous potential to be used for jumping robots because SMA is one of the actuators that have the largest power-to-weight ratio [5].

Motivated by the incorporation of the smart material in a clever robot design, this paper presents the development of a small jumping robot. The design of robot structure is inspired by vertebrates' musculoskeletal system and the jumping mechanism is actuated by SMA wires. The use of SMA for jumping robot is expected to reduce the weight and the complexity of the robot while still maintaining the functions of muscles in jumping.

II. SHAPE MEMORY ALLOY ACTUATOR

The type of SMA used in our work is MMF (Metal Muscle Fiber) SMA wire by NT Research Inc. It is two-way SMA made of titanium and nickel. When it is heated to 70°C, MMF SMA starts to contract. When it is cooled, it relaxes and prolongs its length to the normal state. Although the principle of operation of MMF SMA is based on the applied heat energy, one can operate the SMA by applying the electric energy as well. Instead of heating the material, a suitable amount of electric voltage is applied to the terminals of wire to obtain the same operation. This makes MMF SMA easy to control in many engineering applications. Some essential characteristics of MMF150 SMA wires are summarized in Table 1.

MMF SMA possesses several advantages over conventional actuators. It shows a large ratio of length change. The contracting length is up to 4.5% of its original length. The light weight is another important advantage of SMA. By a simple calculation of the parameters from Table I, one can see that a 200 mm MMF150 wire with the weight of 22.4 mg can contract by 9 mm while carrying the load of 1.8 kg. In other words, it implies that the wire may carry an 80000 times heavier load than its weight while contracting by 9 mm.

The contraction and extension in the longitudinal direction of SMA is similar to the behavior of biological muscles. The contraction time of SMA is a few hundred milliseconds, which satisfies the basic requirement for the jumping action. Our experiments on MMF SMA wires show that 4.5 % of a 200mm wire can be reduced in less than 200 ms, but the elongation takes about 2 seconds.

TABLE I
CHARACTERISTICS OF MMF150 SMA WIRE

Diameter (mm)	Contraction ratio (%)	Applied voltage (V/m)	Tensile Strength (Kgf)	Weight (mg/m)
0.15	4.5	20.7	1.8	112

Manuscript received February 28, 2010. This work was supported by National Research Foundation of Korea Grant funded by the Korean Government (2010-0016534).

Thanhtam Ho and Sangyoon Lee are with the Department of Mechanical Design and Production Engineering, Konkuk University, Seoul, Korea (email: thanhtam.h@gmail.com, slee@konkuk.ac.kr).

III. DESIGN OF THE ROBOT

Studies on human's musculoskeletal system show that the whole movement of lower limbs is realized by nine muscle groups and tendon system combined with the skeleton system as shown in Fig. 1 [6-9]. In order to investigate the human's jumping action, the whole body is divided into four segments. The trunk includes parts in the upper side of the hip. The upper leg or the thigh is the segment between the hip and the knee. The lower leg or the shank is represented by the segment from the knee to the ankle. The plantar part or the foot is the last segment attached at the ankle. The lateral motion in jumping is neglected, and so three joints attached at the hip, the knee, and the ankle are considered as revolute ones.

According to the effects of the muscle on the movement of leg joints, the nine muscle groups in the lower limbs are classified into two muscle types. The first type is called a mono-articular muscle which acts on only one joint. The iliopsoas (ILI), gluteus maximus (GMAX), vastus group (VAS), biceps femoris (BF), tibialis anterior (TA), and soleus (SOL) belong to this type.

The bi-articular muscles, on the other side, are connected to control two joints of the leg. In Fig. 1, the rectus femoris (RF), hamstrings (HAMS), and gastrocnemius (GAS) are three bi-articular muscle groups.

Although it is extremely difficult to understand the functions of each muscle in motions, studies on muscles in human's jumping suggest that both mono-articular and bi-articular muscles contribute to generate the power to lift off the body in the jumping action. Using the experimental data such as the ground reaction force, the cinematographic data, and electromyography data (EMG), the functions of each muscle type in the vertical jumping can become more clear [10-14].

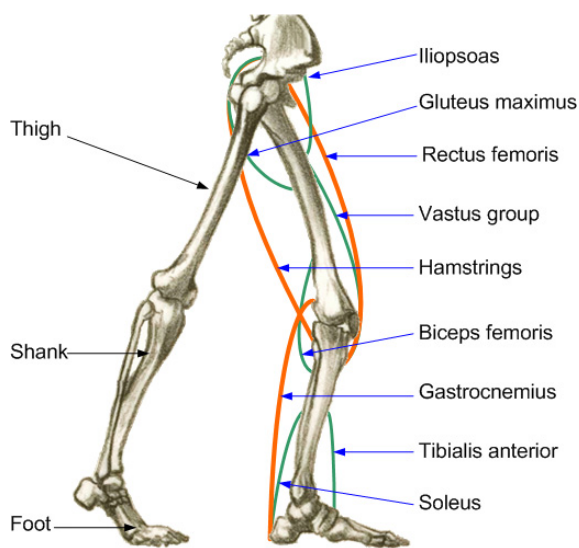


Fig. 1. Human's lower limb musculoskeletal system (adapted from [15]).

It was reported that three mono-articular muscles, VAS, GMAX, and SOL work as the major energy generator for the jumping action [10, 12]. The energy generated by the mono-articular muscles is applied directly to the joint to which the muscles are attached. There is an excess of energy over the amount that is needed at the hip and the knee in some phases of activation. The excess of energy is quite useful if it is transferred to the ankle for the lift-off.

The bi-articular muscles with the ability to act on two joints of the lower limb play a role in this lift-off case. The RF muscle transfers the excess of energy from the hip to the knee while the GAS does the same work from the knee to the ankle. The bi-articular muscles therefore are considered as the energy transporter during jumping. For example, the transferred energy from the knee to the ankle is estimated more than one-fourth of the total energy needed by the ankle during the lift-off. Hence the presence of bi-articular muscle reduces the size and weight of the lower muscle groups. The lower segments of leg can be accelerated more easily as a result. This satisfies the requirements of jumping [10, 16].

The functions of each muscle type in jumping are now clear, and so a proper design and implementation may improve the performance of jumping mechanism significantly. However, mimicking the structure of lower limb musculoskeletal system completely is extremely difficult and complicated. Therefore some degree of modification and simplification is preferred.

Our design aims to simplify the biological structure while keeping the functions of both muscle types as much as possible. In this work, we present a simplified leg model for jumping in which the same number of segments is kept as in the real leg. However the number of muscles is reduced to three and each muscle is to be replaced by an SMA wire. Fig. 2 displays the design concept of the robot leg.

The GMAX muscle is an important energy producer at the hip. The energy generated by GMAX is used by the thigh and the trunk and it is transferred to the knee as well. Therefore the GMAX is kept in the model of jumping robot leg. In Fig. 2, the GMAX is represented by the upper wire that connects the thigh and the body. The GMAX is the only mono-articular muscle in this design.

The other two muscles in Fig. 2 are the bi-articular muscles RF and GAS. Since the RF and GAS muscles are replaced by SMA wires, they are able to contract and stretch to produce the moment at the knee and the ankle, respectively. Hence, these bi-articular muscles are used with two purposes. First, they function as the energy transporter between the joints. Second, they are the energy generator at the knee and the ankle by replacing the mono-articular muscles VAS and SOL (see Fig. 1). Since the number of artificial muscles is reduced significantly, several passive springs are added with the SMA wires at each joint to form the flexor – extensor pairs (see Fig. 2). The major purpose of the antagonistic springs is to recover the robot leg pose after the jump.

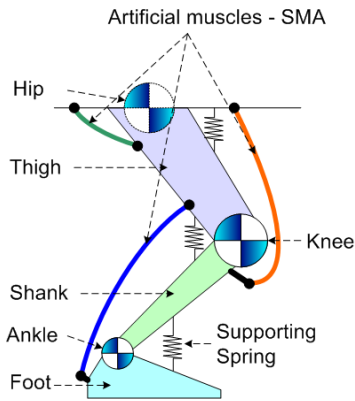


Fig. 2. A simplified design of the robot leg.

In addition to the difficulty with controlling muscles, the landing is another critical issue in the jumping locomotion. Compared to other locomotion ways, the flying phase of jumping is much longer. Besides, the robot is almost uncontrollable during the flying phase. The landing can become unstable as a result. However, the ability to land stably after the flying phase is required for the jumping gait to be a proper locomotion way.

One of the simple methods to increase the stability of the robot in landing is increasing the number of legs [1]. It is also found from the nature that successful jumping vertebrates like a frog and a rabbit use four legs for the jumping. This explains the reason why the jumping robot presented in this paper possesses four legs. The side view of our jumping robot design is illustrated in Fig. 3.

You may notice in Fig. 3 that the rear leg is not identical with the front one. Three DOF on the rear leg corresponds to the hip, the knee, and the ankle controlled by three MMF SMA wires. However each front leg is designed to have two DOF. The foot in each front leg is neglected for the simplification, and the lower part becomes like a flat plate. This design is based on the fact that most skilled jumping vertebrates, a frog for example, have a very small front foot compared to the rear one. Due to this simplification, the whole robot is driven by ten DOF. In other words, ten SMA wires are used to control the jumping action.

In the robot model, the longest segment is 40 mm. It implies that the largest contracting distance can be 1.8 mm since the largest contraction ratio of the MMF SMA is 4.5 %. This amount is not enough to accelerate the joint rotation quickly. Our suggested solution to this problem is using the mechanism named SMA holder shown in Fig. 3. The mechanism consists of several small, lightweight pulleys arranged at two terminals and the SMA is wound around the pulleys. The distance between two pulleys is about 35 mm, and hence the total length can become more than 200 mm with 6 turns of SMA. Since the SMA holders are lightweight and designed to be installed directly to the robot frame, their effect on the robot size and weight is negligible. For instance, the thigh itself in the model is the holder for the SMA wire that represents the GAS muscle (see Fig. 3).

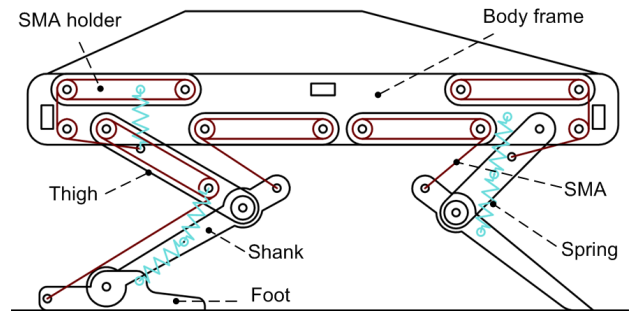


Fig. 3. Model of the four-legged jumping robot.

IV. JUMPING SIMULATION

A. Muscle Coordination for the Jumping

It is obvious that the coordination of muscle activation has a significant effect on the motion. Although it is impossible to figure out fully the activation pattern of the muscles in jumping, studies on the coordination of muscles in jumping agree in the motion sequence of body segments. The early work of Bobbert and his coworkers on human's vertical jumping shows that the motion of trunk part is started first, 330 ms before the lift-off of the toes. Then the motions of thigh and shank are initialized 270 ms and 220 ms before the lift-off, respectively. The foot is found to change its joint angle at about the same time with a trunk. However, its significant change is started just 150 ms before the lift-off moment [10]. A similar pattern in the rotation of the foot, the thigh, and the shank can be found in other reports on muscle behaviors in the jumping action [11-13, 17].

Although the motion sequence of body segments in jumping is not directly related to the coordination of muscle activation, it shows the clue to find how to activate the muscles in a sequence to obtain the desired jumping. Unfortunately, the general pattern of muscle activation in the jumping action is still not clearly understood. Among the possible methods to determine the activation sequence of muscles, the parametric simulation may be one of the most useful and reliable methods. Our computer simulation work is explained in the following subsection.

B. Simulation of the Jumping Robot

Since the major purpose of our simulation work is to determine a particular sequence of muscle activation in the vertical and forward jumping of the four-legged robot, the lateral movement can be neglected. With this assumption, one is able to consider the jumping robot as a 2-D model with one rear leg and one front leg attached to the body frame. The simulation work was conducted using the Working Model 2D software. The 2-D equivalent model of the robot is built to have the same configuration as the design shown in Fig. 3. Fig. 4 displays the equivalent model.

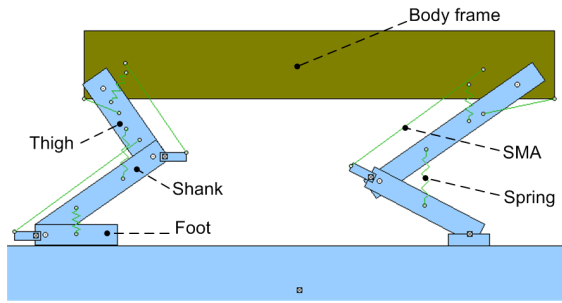


Fig. 4. Simulation model of the four-legged jumping robot.

The weight of the robot is about 70 gram, of which 20% is the mass of the robot legs. For the rear leg, the length of thigh, shank and foot are 35 mm, 40 mm, and 25 mm respectively. The upper leg on front leg is 55 mm long while the lower one is 40 mm. The spring stiffness is chosen to be small, 0.01 N/mm. The small stiffness reduces the resistance force during the jumping activation. The simulation is performed on the floor with a large friction coefficient, 1. This condition prevents the robot from slipping on the floor.

The SMA wires in the design are represented by the rope elements in the simulation. Before starting the implementation of simulation it is important to select a suitable model for the SMA wire. Our experiments with 200 mm MMF150 SMA wire show that the wire needs just 150 ms to obtain the maximum contraction, which is 9 mm. Since the contraction time of SMA is quite short, it is reasonable to approximate the contraction to a reduced first order polynomial or a line with the maximum magnitude of 9 mm. The slope of line corresponds to the contraction speed of the wire.

The activation of SMA wires in the simulation is performed mainly based on the pattern of rotation of each segment in jumping as described in the previous subsection. Unfortunately, the activation sequence to produce the rotation pattern is not unique. A parametric study is applied to execute the simulation. In this simulation, the parameter is the sequence of activating the SMA wires. A set of input parameters is also selected for the simulation.

One of the activation sequences that produces a good result is shown in Table II. This sequence not only agrees with the segment's rotation pattern but also produces the highest and farthest jumping. The SMA wires are numbered from top to bottom and from left to right. For example, SMA1 denotes the upper SMA wire on the rear leg in Fig. 4. The time in the table means the moment when the SMA wire is activated. The stating time, 0 ms, is the moment when both toes lift off the ground. The speed in the table indicates the contraction speed of the SMA wire.

One can observe from the table that the GMAX and RF SMA are activated earlier than the GAS SMA by 50 ms, but the contraction speed of the former SMA wires is much slower than that of the latter. This guarantees that the motion of foot segment is started after the others and the speed of foot segment is increased quickly right before the lift-off of the rear toe.

TABLE II
ACTIVATION SEQUENCE OF THE SMA WIRES

	SMA1	SMA2	SMA3	SMA4	SMA5
Time (ms)	-150	-150	-100	-130	-80
Speed (mm/s)	20	20	70	20	90

If a similar activation sequence is applied to the front leg, the robot should be able to perform a vertical jumping. However, in order to obtain a forward jumping, another constraint is required, which is the time gap between the front leg and the rear one. One can notice in Table II that each SMA in the front leg is activated 20 ms later than the corresponding one in the rear leg.

As a result, while the rear SMA wires are activated, the front ones are not activated yet. When only the rear legs are extended, the motion of robot body can be modeled as the rotation around the temporary center at the end of the front leg (see Fig. 5). The center of mass of the robot is accelerated to move forward and upward. This motion continues until the motion of front leg is started. As the motion of front leg is added to the current motion of the center point, the robot can move forward as a result.

From the simulation, we found that the center of robot can reach the maximum height of 45 mm and move forward by 35 mm for each jumping step. This result implies that the maximum jumping height is about 70% half of its height and the maximum distance per jumping is about 25% of its length. In addition to the jumping height and distance, the rotation angle of each segment of the rear leg is measured as shown in Fig. 6. Note in Fig. 6 that the time origin is set at the moment when the robot starts the flying phase. Since the rear toe lifts off the ground about 30 ms earlier than the front one, the data after the lift-off moment of the rear toe is not considered (the shadow area). The change in the thigh angle, the shank angle, and the foot angle are represented by the thin solid line, the dashed line, and the thick solid line, respectively. One can find that the activation sequence and time of each angle in the simulation matches Bobbert's data [10]. The rotations of the thigh and the shank are started first. In case of the foot angle, a significant change is found at -90 ms, which is about the half of the time period from the first motion of body part to the lift-off moment of the rear toe.

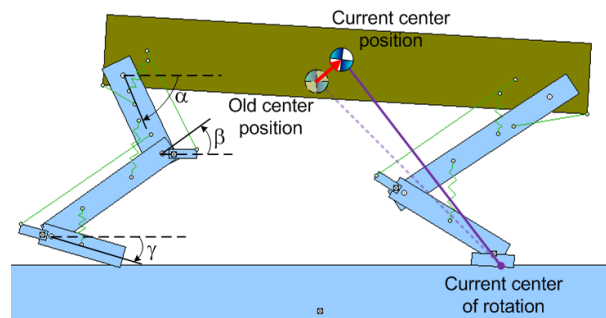


Fig. 5. Motion of the rear leg and the center of mass.

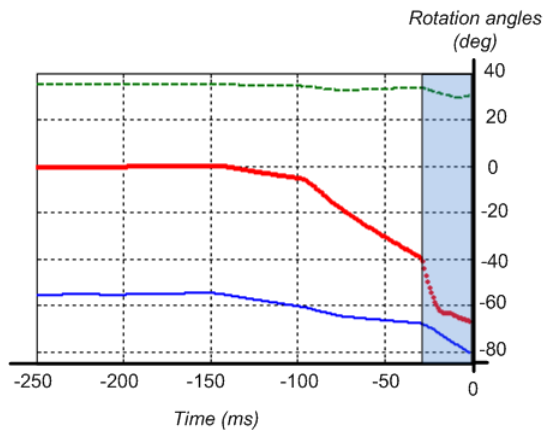


Fig. 6. The rotation angles of the segments on the rear leg before lifting-off: the thigh angle - α (light solid line), the shank angle - β (dash line) and the foot angle - γ (heavy solid line).

V. PROTOTYPE AND EXPERIMENTS

Based on the robot design in Sec. II, a prototype of the jumping robot has been fabricated, as shown in Fig. 7. Acrylic is mostly used to make the leg segments as well as the body frame. Each part was designed with AutoCAD and fabricated using a CNC machine. Lightweight pulleys are utilized to form the SMA holders. Each MMF150 SMA wire is about 200 mm long and is wound around the pulleys. Ten springs with a low stiffness are inserted to form the flexor-extensor pairs with the SMA wires. The length, width, and height of the prototype are 150 mm, 65 mm, 65 mm, respectively. The weight of the legs takes about 20 % of the total weight, which is 80 gram.

In our experiments with the prototype, the muscle activation scheme obtained through the simulation is applied in the same way (see Table II for more details). Since any transverse motion is not desired in the experiments, each pair of symmetrical SMA wires is controlled by one signal. Therefore five control lines are needed to control ten SMA wires. The control work is done off-board by an external control circuit.

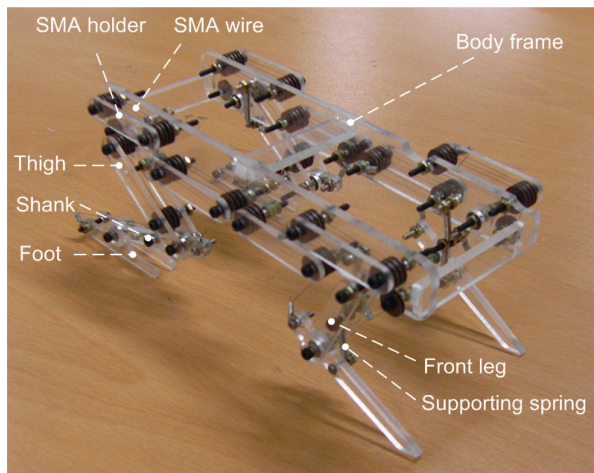


Fig. 7. The jumping robot prototype.

Before explaining the experimental results, it is essential to understand how the contraction period of time and speed of SMA wire are controlled. Fig. 8 illustrates the signals which are used to control the SMA wire. In order to increase the contraction speed of 200 mm MMF150 SMA wire, we used the electric voltage of 24 V. This is about 4 times larger than the normal voltage, which is 20.7 V/m as specified in Table I. Applying a large voltage constantly may cause the SMA wire to burn. But we can avoid the problem by using the short-time pulse activation.

The width of pulse in Fig. 8(b) defines the contraction period of the SMA wire. We can also control the contraction speed that may be different for wires, by using another signal named pulse width modulation (PWM) signal in Fig. 8(a). If the high-frequency PWM signal whose pulse width can control the contraction speed is mixed with the pulse signal, we obtain the control signal for each SMA wire, as shown in Fig. 8(c).

All the jumping experiments were conducted on the plywood plate and the off-board control circuit was used to control the SMA wires. We used the same sequence to activate the SMA wires as in Table II. By this setting, the robot can jump forward by 25 mm in each jump. This result is comparable to the simulation result. The total period of time from the start of jumping to the landing is about 3 sec in which the elongating time of SMA wire takes more than 90%. Three snapshots of the jumping experiment are displayed in Fig. 9. The frame #1 shows the robot before it starts jumping. The flying phase is shown in frame #2 and the landing moment is captured in frame #3.

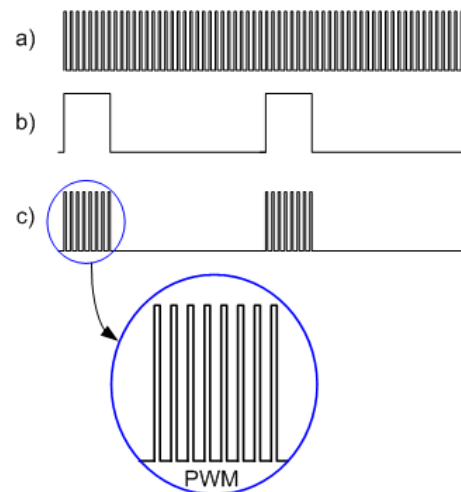


Fig. 8. Control signal for SMA wires: (a) primary PWM signal, (b) pulse signal, and (c) control signal.

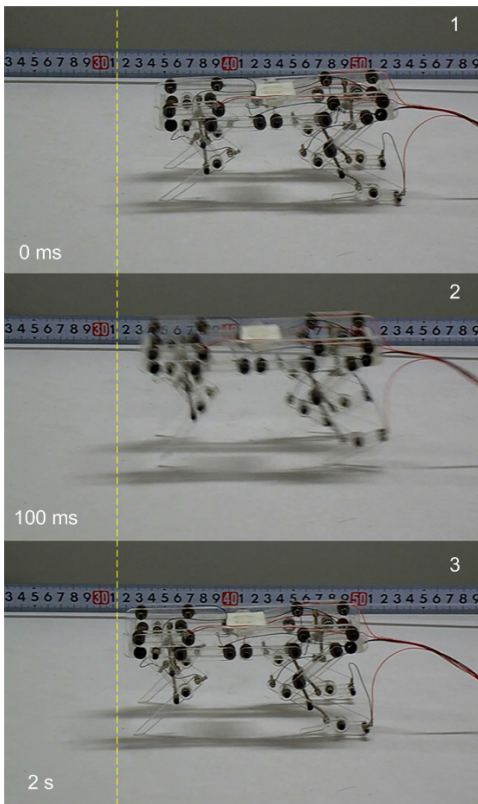


Fig. 9. Snapshots of the robot prototype in jumping.

VI. CONCLUSION

We presented the development of four-legged jumping robot that is actuated by SMA wires only. The design of robot is inspired from vertebrates' musculoskeletal system. The functions of mono-articular and bi-articular muscle types are studied carefully and applied in the simplified fashion. The four-leg configuration robot is chosen to increase the stability of the system during the landing after the flying phase. The rear leg is designed to have three segments that correspond to the thigh, the shank, and the foot. Among nine primary muscle groups, three are selected to implement on the robot. This simplifies the size and weight of the robot and reduces the complexity of the robot. But the functions of each essential muscle type are still maintained. Through the parametric simulation, a particular pattern of activation for muscles groups is determined. The parameters obtained from the simulation are applied to a robot prototype in experiments. The forward distance obtained from the jumping experiment is comparable to the simulation result. The experiments with 50 gram load on the robot with the same activation scheme yielded the same result in terms of the forward distance. This suggests a simple way to improve the performance of jumping robot by developing a superior sequence of SMA activation, which needs more diverse research on biomimetics and parametric simulation work.

- [1] P. González-de-Santos, E. Garcia, and J. Estremera, *Quadrupedal Locomotion: An Introduction to the Control of Four-legged Robots*, Springer, 2005.
- [2] K. Arikawa and T. Mita. "Design of multi-DOF jumping robot", *Proc. of IEEE International Conference on Robotics and Automation*, vol. 4, 2002, pp. 3992-3997.
- [3] R. Niiyama, A. Nagakubo, and Y. Kuniyoshi, "Mowgli: A Bipedal Jumping and Landing Robot with an Artificial Musculoskeletal System", *Proc. of IEEE International Conference on Robotics and Automation*, Roma, Italia, April, 2007, pp. 2546 - 2551.
- [4] T. Oshima, N. Momose, K. Koyanagi, T. Matsuno, and T. Fujikawa, "Jumping Mechanism Imitating Vertebrate by the Mechanical Function of Bi-articular Muscle". *International Conference on Mechatronics and Automation*, 2007, pp. 1920-1925.
- [5] C. Mavroidis, "Development of advanced actuators using Shape Memory Alloys and Electrorheological Fluids", *Research in Nondestructive Evaluation*, vol. 14, 2002, pp. 1-32, March.
- [6] T. Spagele, A. Kistner, and A. Gollhofer, "Modelling, simulation and optimisation of a human vertical jump", *Journal of Biomechanics*, vol. 32, 1999, pp. 521-530.
- [7] A. Guyton and J. Hall, *Textbook of Medical Physiology*, 11th ed., Philadelphia: Elsevier Saunders, 2005.
- [8] V. D. Graaff, *Human Anatomy*, 6th ed., New York: McGraw-Hill, 2001.
- [9] S. S. Mader, *Understanding Human Anatomy and Physiology*, New York: McGraw-Hill, 2004.
- [10] M. F. Bobbert and G.J. van Ingen Schenau, "Coordination in vertical jumping", *Journal of Biomechanics*, vol. 21, 1988, pp. 249-262.
- [11] M. G. Pandy, F. E. Zajac, E. Sim, and W. S. Levine, "An optimal control model for maximum-height human jumping", *Journal of Biomechanics*, vol. 23, pp. 1185-1198, 1990.
- [12] M. G. Pandy, and F.E. Zajac, "Optimal muscular coordination strategies for jumping", *Journal of Biomechanics*, vol. 24, 1991, pp. 1-10.
- [13] F. E. Zajac, "Muscle coordination of movement: A perspective", *Journal of Biomechanics*, vol. 26, 1993, pp. 109-124.
- [14] M. F. Bobbert, "The effect of coordination on vertical jumping performance", in *20th International Symposium on Biomechanics in Sports*, Cáceres, Spain, 2002.
- [15] M. Langeneckert, *The Human Machine: Art and Anatomy*. Available: <http://shutupanddrawblogspotcom.blogspot.com>.
- [16] M. F. Bobbert, P. A. Huijing, and G. J. van Ingen Schenau, "An estimation of power output and work done by the human triceps surae muscle-tendon complex in jumping", *Journal of Biomechanics*, vol. 19, 1986, pp. 899-906.
- [17] M. F. Bobbert, W. W. de Graaf, J. N. Jonk, and L. J. Richard Casius, "Explanation of the bilateral deficit in human vertical squat jumping", *J. Appl. Physiol.*, vol. 100, 2006, pp. 493-499.